COORDINATION COMPOUNDS

Hydrates of Lanthanide(III) 2-Thiobarbiturates: Synthesis, Structure, and Thermal Decomposition

N. N. Golovnev[a], *, M. S. Molokeev[a, b, c], M. K. Lesnikov[a], and A. S. Samoilo[a]

[a]Siberian Federal University, Krasnoyarsk, 660041 Russia
[b]Kirenskii Institute of Physics, Federal Research Center "Krasnoyarsk Scientific Center,"
Siberian Branch, Russian Academy of Sciences, Krasnoyarsk, 660036 Russia
[c]Far Eastern State Transport University, Khabarovsk, 680021 Russia
*e-mail: ngolovnev@sfu-kras.ru

Abstract—The hydrates $Ln(Htba)_3 \cdot 3H_2O$ (Ln = Yb **(I)**, Er **(II)**, Ho **(III)**; H_2tba = 2-thiobarbituric acid), $Ln(Htba)_3 \cdot 2H_2O$ and $Ln(Htba)_3 \cdot 8H_2O$ were crystallized from aqueous solutions. According to single-crystal X-ray diffraction analysis data, the structure of monoclinic crystals of isostructural complexes **I–III** was $[Ln_2(H_2O)_6(\mu_2\text{-}Htba\text{-}O,O')_4(Htba\text{-}O)_2]_n$. The formation of isostructural $Ln(Htba) \cdot 2H_2O$ (Ln = La, Ce, Eu, Yb, Lu), $Ln(Htba)_3 \cdot 8H_2O$ (Ln = Eu, Tb, Ho, Yb) and $Y(Htba)_3 \cdot nH_2O$ (n = 2, 8) was confirmed by the comparison of X-ray diffraction patterns, and their composition was determined by elemental and thermal analyses. The stability of crystal hydrates under heating in an air atmosphere and in contact with their saturated solutions was studied.

Keywords: lanthanides(III), thiobarbiturates, hydrates, structure, stability

INTRODUCTION

Thiobarbituric acid (H_2tba) as a polyfunctional N,N',O,O',S-donating ligand with various binding centers (Fig. 1) forms coordination polymers of diverse structures with metal ions [1, 2]. Noteworthy are neutral homogeneous complexes (NHCs) with ligands of only one sort and water molecules, as they do not contain counterions, which frequently fill the potentially useful channels or cavities in the crystal lattice. Taking into account the various coordination modes of $Htba^-$ ions and H_2O molecules (Table S1) [3] in the crystallization of NHCs from an aqueous medium, it is possible to obtain several compounds with a different number of coordinated water molecules. We have synthesized hydrates of HNCs with thiobarbituric, barbituric (H_2ba), and 1,3-diethyl-2-thiobarbituric (HDetba) acids and *s*-, *p*-, and *d*-metal ions (Table S1) [2, 3]. It is of interest to study the structural and hydrate variety of compounds of this class for the practically important rare-earth elements (REEs) [4−7]. The information about the synthesis, structure, and properties of REE thiobarbiturate complexes, which may have luminescent properties and serve as precursors for the synthesis of oxysulfates [8] and oxides [9], is limited by five isostructural compounds $Ln(Htba)_3 \cdot 3H_2O$ [9]. In the present work, the hydrates $Ln(Htba)_3 \cdot 3H_2O$, $Ln(Htba)_3 \cdot 2H_2O$,

$Ln(Htba)_3 \cdot 8H_2O$ and $Y(Htba)_3 \cdot nH_2O$ (n = 2, 8) were synthesized. They were studied by powder X-ray diffraction and thermal analysis. The structures of $Ln(Htba)_3 \cdot 3H_2O$ (Ln = Yb **(I)**, Er **(II)**, Ho **(III)**) were characterized by X-ray diffraction. Only one crystal structure was characterized for each NHC [10].

EXPERIMENTAL

$LuCl_3 \cdot 6H_2O$, $YbCl_3 \cdot 6H_2O$, Er_2O_3, Ho_2O_3, $YCl_3 \cdot 6H_2O$, $Eu(CH_3COO)_3 \cdot 4H_2O$, $TbCl_3 \cdot 6H_2O$, $GdCl_3 \cdot 6H_2O$, $CeCl_3 \cdot 7H_2O$, $La(NO_3)_3 \cdot 6H_2O$, H_2tba, HCl, and NaOH (all of chemically pure grade) were used for synthesis without additional purification. The oxides Er_2O_3 and Ho_2O_3 were dissolved in concen-
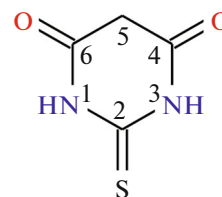
Fig. 1. Graphical formula for a 2-thiobarbituric acid (H_2tba) molecule.

Table 1. Elemental analysis results for the synthesized compounds

Short formula	Bulk formula	Content of elements found/calcd., wt %			
		C	H	N	S
Yb(Htba)$_3$ · 3H$_2$O	C$_{12}$H$_{15}$N$_6$O$_9$S$_3$Yb	22.42/21.95	2.17/2.30	13.04/12.80	14.90/14.65
Er(Htba)$_3$ · 3H$_2$O	C$_{12}$H$_{15}$ErN$_6$O$_9$S$_3$	22.29/22.15	2.12/2.32	13.20/12.91	15.01/14.78
Ho(Htba)$_3$ · 3H$_2$O	C$_{12}$H$_{15}$HoN$_6$O$_9$S$_3$	22.48/22.23	2.20/2.33	13.35/12.96	15.12/14.84
La(Htba)$_3$ · 2H$_2$O	C$_{12}$H$_{13}$LaN$_6$O$_8$S$_3$	23.53/23.85	1.90/2.17	13.78/13.90	15.43/15.92
Ce(Htba)$_3$ · 2H$_2$O	C$_{12}$H$_{13}$CeN$_6$O$_8$S$_3$	24.01/23.80	2.06/2.16	14.16/13.88	16.11/15.89
Eu(Htba)$_3$ · 2H$_2$O	C$_{12}$H$_{13}$EuN$_6$O$_8$S$_3$	22.94/23.34	2.30/2.12	13.39/13.61	15.42/15.58
Yb(Htba)$_3$ · 2H$_2$O	C$_{12}$H$_{13}$N$_6$O$_8$S$_3$Yb	23.06/22.57	1.87/2.05	13.45/13.16	15.44/15.07
Lu(Htba)$_3$ · 2H$_2$O	C$_{12}$H$_{13}$LuN$_6$O$_8$S$_3$	22.22/22.51	2.01/2.05	12.76/13.12	14.63/15.02
Y(Htba)$_3$ · 2H$_2$O	C$_{12}$H$_{13}$N$_6$O$_8$S$_3$Y	25.84/26.00	2.17/2.36	15.56/15.16	17.67/17.35
Eu(Htba)$_3$ · 8H$_2$O	C$_{12}$H$_{25}$EuN$_6$O$_{14}$S$_3$	20.15/19.87	3.30/3.47	11.69/11.58	13.56/13.26
Tb(Htba)$_3$ · 8H$_2$O	C$_{12}$H$_{25}$N$_6$O$_{14}$S$_3$Tb	19.97/19.68	3.56/3.44	11.32/11.47	13.10/13.13
Ho(Htba)$_3$ · 8H$_2$O	C$_{12}$H$_{25}$HoN$_6$O$_{14}$S$_3$	19.32/19.52	3.63/3.41	11.16/11.38	12.74/13.03
Yb(Htba)$_3$ · 8H$_2$O	C$_{12}$H$_{25}$N$_6$O$_{14}$S$_3$Yb	19.66/19.31	3.21/3.38	11.67/11.26	13.28/12.89
Y(Htba)$_3$ · 8H$_2$O	C$_{12}$H$_{25}$N$_6$O$_{14}$S$_3$Y	22.33/21.76	3.57/3.80	12.89/12.67	14.76/14.52

trated HCl and then carefully evaporated to dry chloride salts.

Synthesis of Ln(Htba)$_3$ · 3H$_2$O (Ln = Yb (I), Er (II), Ho (III)). Hydrates of lanthanide salts (0.11 mmol) were dissolved in water (10 mL) to add solid H$_2$tba (0.05 g, 0.35 mmol), thereupon the mixture was neutralized with a 1 M NaOH solution to pH of 4. The formed fine-crystalline precipitates composed, according to X-ray diffraction data, predominantly of corresponding octahydrates were dissolved under heating in a great excess of distilled water (200–300 mL), and the solutions allowed to vaporize for several weeks at room temperature to the formation of crystals suitable for X-ray diffraction analysis. The yield of complexes **I–III** increased during the evaporation of water to attain 20–30% at a water volume of 100–150 mL. The elemental analysis results for complexes **I–III** are given in Table 1.

A key factor influencing the composition of the synthesized isostructural hydrates M(Htba)$_3$ · 2H$_2$O and M(Htba)$_3$ · 8H$_2$O (M = Ln, Y) is the temperature. As a rule, the interaction between a REE salt and a NaOH neutralized H$_2$tba solution (pH 4–5) leads to the formation of colorless octahydrates M(Htba)$_3$ · 8H$_2$O at room temperature and pale yellow dihydrates M(Htba)$_3$ · 2H$_2$O at 90°C. The methods of their synthesis are described below in the general form.

Synthesis of M(Htba)$_3$ · 2H$_2$O (M = La, Ce, Eu, Yb, Lu, Y). To H$_2$tba (0.20 g, 1.4 mmol) in water (5 mL), NaOH (0.056 g, 1.4 mmol) was added, thereupon the mixture was allowed to stand at 90°C for 5 min to the complete dissolution of thiobarbituric

acid. To the hot yellow-orange solution, an aqueous solution (1 mL) containing a M(III) salt (0.46 mmol) was added under stirring. The initially formed white bulky precipitate (M(Htba)$_3$ · 8H$_2$O) became more compact and yellow in color. It was filtered out, washed with acetone (2 mL), and dried in the air to a constant weight. The yield of these compounds was 40–50%. The results of their elemental analysis agree with the proposed composition (Table 1).

Synthesis of M(Htba)$_3$ · 8H$_2$O (M = Eu, Tb, Ho, Yb, Y). The methods for the synthesis of these isostructural compounds differ from the previous technique in that their synthesis was performed at room temperature, and a small excess of NaOH (1.6 mmol) was used for the faster dissolution of 2-thiobarbituric acid. The yield of these compounds was 50–60%. Their composition was confirmed by the chemical analysis data (Table 1).

X-ray diffraction analysis. Yellow crystals oc complex **I** (Ln = Yb) of 0.3 × 0.3 × 0.2 mm in size, complex **II** (Ln = Er) of 0.35 × 0.35 × 0.3 mm in size, and complex **III** (Ln = Ho) of 0.3 × 0.2 × 0.2 mm in size were studied at 296 K. Reflection intensities were measured on a Bruker AXS SMART APEX II single-crystal diffractometer (MoK_α radiation) with a CCD detector. The experimental absorption corrections were applied with the SADABS software [11] by multiscanning. The structural model was established by direct methods and refined with the SHELXTL software suite [12]. Electron density difference syntheses were used to determine the hydrogen atom positions, which were further idealized and refined as bonded with the basic atoms. X-ray diffraction experiment

Table 2. Parameters of X-ray diffraction experiment and refinement details for the structures of complexes **I−III**

Parameter	Value		
Crystal	**I**	**II**	**III**
Bulk formula	$C_{24}H_{30}N_{12}O_{18}S_6Yb_2$	$C_{24}H_{30}Er_2N_{12}O_{18}S_6$	$C_{24}H_{30}Ho_2N_{12}O_{18}S_6$
FW	1313.04	1301.48	1296.82
Space group, Z	$P2/n$, 2	$P2/n$, 2	$P2/n$, 2
a, Å	13.9302 (4)	13.9848 (6)	13.9917 (9)
b, Å	9.9688 (3)	10.0106 (4)	10.0182 (7)
c, Å	15.4215 (5)	15.4161 (6)	15.3907 (10)
β, deg	109.4421 (7)	109.541 (1)	109.6202 (16)
V, Å^3	2019.43 (11)	2033.89 (14)	2032.1 (2)
ρ_{calcd}, g/cm^3	2.159	2.125	2.119
μ, mm^{-1}	5.002	4.495	4.262
Reflections in total	29917	44856	20957
$2\theta_{max}$, deg	61.938	78.088	53.004
Independent reflections N_1 (R_{int})	6426 (0.0638)	11253 (0.0410)	4205 (0.0989)
Number of reflections with $F > 4\sigma(F)$, N_2	5006	9307	2964
Range of indices h, k, l	$-20 \le h \le 20$, $-14 \le k \le 14$, $-22 \le l \le 22$	$-24 \le h \le 24$, $-17 \le k \le 17$, $-26 \le l \le 26$	$-17 \le h \le 17$, $-12 \le k \le 12$, $-19 \le l \le 19$
Weighting scheme for F^2	$w = 1/[\sigma^2(F_o^2) + (0.0167P)^2 + 5.348P]$	$w = 1/[\sigma^2(F_o^2) + (0.0162P)^2 + 2.9638P]$	$w = 1/[\sigma^2(F_o^2) + (0.0205P)^2 + 8.8779P]$
	$P = \max(F_o^2 + 2F_c^2)/3$		
Numer of refined parameters	299	299	299
R (for N_1 reflections)	0.0532	0.0506	0.0732
R (for N_2 reflections)	0.0318	0.0368	0.0394
$wR(F^2)$ (for N_1 reflections)	0.0741	0.0654	0.0903
$wR(F^2)$ (for N_2 reflections)	0.0625	0.0618	0.0732
GOOF	1.068	1.011	1.033
Extinction coefficient	Not refined		
$(\Delta/\sigma)_{max}$	<0.001	<0.001	<0.001
$\Delta\rho_{max}/\Delta\rho_{min}$, e/Å^3	1.580/−2.535	1.196/−2.980	1.598/−1.308

parameters and structure refinement results are given in Table 2. The structures of complexes **I−III** were deposited with the Cambridge Structure Database (nos. 1971780−1971782; deposit@ccdc.cam.ac.uk or http://www.ccdc.cam.ac.uk/data_request/cif).

The powder X-ray diffraction patterns of these complexes were recorded at room temperature on a Bruker D8 Advance diffractometer with a Vantec linear detector and CuK_α radiation. The phase purity of powders of complexes **I−III** was confirmed with the use of unit cell parameters from the single-crystal experiment, and the profile of refining the unit cell parameters was fitted by the Le Bail method using the TOPAS 4.2 software [13]. Refinement was stable and gave good difference X-ray diffraction patterns (Fig. 2).

The thermal analysis of the complexes was performed on a TA Instruments SDT-Q600 analyzer in an air flow (50 mL/min) within a range of 22−850°C at a heating rate of 10 K/min. The composition of gaseous products was determined on a Thermo Scientific
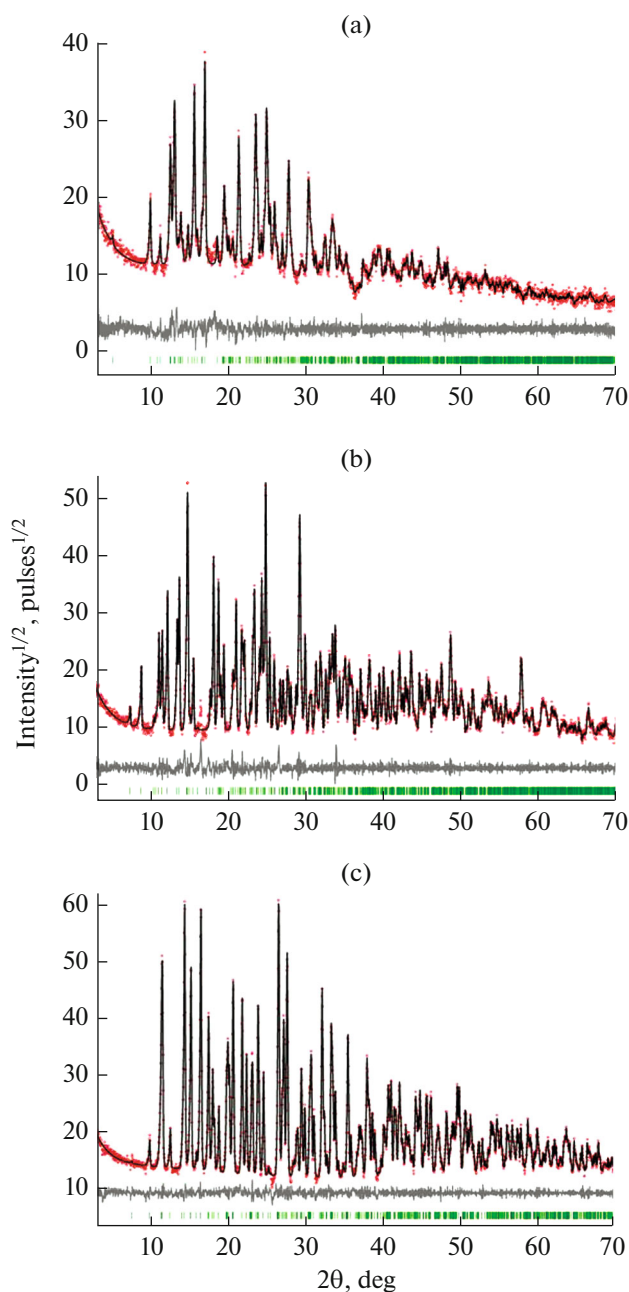
Fig. 2. Experimental, theoretical, and difference X-ray diffraction patterns for crystals of (a) $Y(Htba)_3 \cdot 8H_2O$, (b) $Ho(Htba)_3 \cdot 3H_2O$, and (c) $Yb(Htba)_3 \cdot 2H_2O$.

Nicolet380 IR spectrometer integrated with a thermal analyzer.

RESULTS AND DISCUSSION

The formation of three groups of hydrates $M(Htba)_3 \cdot 8H_2O$, $M(Htba)_3 \cdot 3H_2O$ and $M(Htba)_3 \cdot 2H_2O$ agrees with the results of chemical and thermal analyses. An isostructural character of the hydrates with the same chemical composition is confirmed by the coincidence of their powder X-ray diffraction patterns and calculated crystallographic parameters (Tables 2−4). For comparison Fig. 2 shows experimental X-ray diffraction patterns, which appreciably differ from each other, for three hydrates of REE thiobarbiturates with different compositions.

Crystallization from aqueous solution at room temperature primarily results in white bulky $M(Htba)_3 \cdot 8H_2O$ hydrates, which are then converted into $M(Htba)_3 \cdot 3H_2O$ for 1−3 months at room temperature. At 90°C, $M(Htba)_3 \cdot 8H_2O$ is usually converted into more compact yellow fine-crystalline $M(Htba)_3 \cdot 2H_2O$ precipitates. Such transformations agree with the empirical rule according to which the compounds containing a smaller number of water molecules crystallize at a higher temperature. All our attempts to separate these complexes in the form of crystals suitable for single-crystal X-ray diffraction analysis were unsuccessful. When brough in contact with the mother solution for 1−3 months at room temperature, $M(Htba)_3 \cdot 2H_2O$ crystals were partially converted into the hydrates $M(Htba)_3 \cdot 3H_2O$, which were more thermodynamically stable in an aqueous solution.

The independent part of a cell in isostructural $Ln(Htba)_3 \cdot 3H_2O$ (Ln = Yb, Er, Ho) contains two Ln^{3+} and three $Htba^-$ ions and three water molecules in shared positions. The coordination of $Htba^-$ ions to Ln^{3+} ions is implemented only through O atoms. One of the Ln^{3+} ion is bonded with six $Htba^-$ ions (two terminal and four bridging ones) and two water molecules, and the other is linked to four bridging $Htba^-$ ions and four water molecules (Fig. 3). The $Ln(1)O_8$ and $Ln(2)O_8$ polyhedra are square antiprisms linked to each other by means of bridging $Htba^-$ ions with the formation of an infinite layer in the plane perpendicular to direction $a + c$ (Fig. S1). Taking into account the different coordination environments of two independent Ln^{3+} ions and the fact that the structure contains both μ_2-bridging and terminal $Htba^-$ ligands, the structure of the considered complexes can be described best of all by the formula $[Ln_2(H_2O)_6(Htba-O,O')_4(Htba-O)_2]_n$ (Fig. 3) or merely $Ln_2(H_2O)_6(Htba)_6$. They are isostructural to the earlier characterized compounds $Eu_2(Htba)_6(H_2O)_6$ [8], $Sm_2(Htba)_6(H_2O)_6$, and $Ln_2(Htba)_6(H_2O)_6$ (Ln = Tb, Gd, Nd) [9]. The Ln−O bonds (Table S2) in complexes **I**−**III** (2.263(3)−2.406(3) Å) have typical lengths [10] and naturally decrease from complex **I** to complex **III**. The structure contains three independent, one terminal (C), and two bridging (An ad B) $Htba^-$ ions. Their corresponding geometric parameters are in satisfactory agreement with the literature data [11−19] and almost coincide with each other for complexes **I**−**III**, e.g., the lengths of the bonds C−O (1.250(8)−1.274(8) Å), C(4)−C(5) and C(5)−C(6) (1.382(10)−1.402(6) Å), and C−S (1.664(4)−1.697(7) Å).

Table 3. Crystallographic parameters of $Ln(Htba)_3 \cdot 8H_2O$ (space group $P\overline{1}$)

Metal	a, Å	b, Å	c, Å	α, β, γ, deg	V, Å^3
Eu	7.794(1)	9.169(1)	18.448(2)	97.25(1), 91.72(1), 112.18(1)	1206.8(2)
Tb	7.789(3)	9.152(4)	18.458(7)	97.14(2), 91.76(2), 112.15(3)	1205.0(8)
Ho	7.769(1)	9.128(1)	18.434(2)	97.07(1), 91.78(1), 112.21(2)	1169.9(3)
Yb	7.781(1)	9.152(1)	18.458(2)	97.14(1), 91.76(1), 112.15(2)	1204.0(2)
Y	7.764(3)	9.120(4)	18.411(8)	97.08(2), 91.69(2), 112.27(3)	1193.1(9)

Structural analysis showed that complexes **I–III** have twelve hydrogen bonds N−H···O, N−H···S, O−H···O, and O−H···S (Table S3) with participation of all the Htba$^-$ ions and water molecules. These hydrogen bonds form a three-dimensional framework, in which the supramolecular $R_2^2(8)$, $S(6)$, $R_2^2(28)$, and $R_4^4(26)$ motifs can be distinguished [20] similarly to the other isostructural Ln(III) thiobarbiturates [8, 9]. The π–π interactions [21] between Htba$^-$ ions (Table S4) of head-to-tail type additionally stabilize the structure of the complexes.

At the beginning of thermal decomposition, all the synthesized hydrates are subjected to complete dehydration confirmed by the results of the IR spectroscopic analysis of gaseous products. We have not managed to identify the crystalline phases formed upon the complete dehydration of the synthesized compounds using X-ray diffraction. The compositions of intermediate and final thermolysis products were not studied in this work. The dehydration of $Y(Htba)_3 \cdot 8H_2O$ occurs in two stages; the first begins at ~80°C, and the second is started at ~100°C (Fig. 4a). They are accompanied by the appearance of endotherms at 85 and 129°C, respectively. The weight loss (Δm_{exp}) at ~200°C is close to its theoretically calculated value (Δm_{calcd}) under the assumption of complete dehydration (Δm_{exp} = 20.9%, Δm_{calcd} = 21.7%, −8H$_2$O). At $T > 370$°C, the sample sustains oxidative decomposition, which corresponds to two exotherms at 422 and 598°C on the DSC curve. According to the results of IR spectroscopic analysis of gaseous products, water is the only gaseous product below 370°C, and CO$_2$, CS$_2$, and NH$_3$ were detected among the thermolysis products within a range of 380−800°C.

As follows from Fig. 4b, the dehydration of $Ho(Htba)_3 \cdot 3H_2O$ (**III**) begins at 180°C and ends at 270−280°C. The experimental weight loss is close to the calculated value under the assumption of the removal of all H$_2$O molecules (Δm_{exp} = 7.97%, Δm_{calcd} = 8.33%, −3H$_2$O). Dehydration is accompanied by the appearance of an endotherm at 234°C. At $T > 320$°C, the sample sustains oxidative decomposition, which corresponds to the exotherm at 570°C on the DSC curve. Below 320°C, the only gaseous product is water, and CS$_2$, NH$_3$, SO$_2$, and CO$_2$ were revealed in

the thermolysis products within a range of 380−800°C.

The dehydration of $Yb(Htba)_3 \cdot 2H_2O$ begins at 230°C and almost terminates at 300°C (Fig. 4c). It corresponds to the endotherm at 237°C. The weight loss at 250°C exceeds the theoretically calculated value under the assumption of the complete dehydration of this compound (Δm_{exp} = 6.48%, Δm_{calcd} = 5.64%, −2H$_2$O). The observed difference seems to be due to a hygroscopic of this compound. At $T > 370$°C, the organic ligand is subject to oxidation, which corresponds to the strong exotherm at 451°C in the DSC curve. At $T < 370$°, the only gaseous product is water, and CS$_2$, NH$_3$, SO$_2$, and CO$_2$ were revealed among the thermolysis products within a range of 380−800°C.

The removal of all the water molecules from $Y(Htba)_3 \cdot 8H_2O$ occurring as soon as at $T < 150$°C allows us to classify them as crystallization molecules. In contrast to them, the water molecules in $Ho(Htba)_3 \cdot 3H_2O$ and $Yb(Htba)_3 \cdot 2H_2O$ are most likely to be coordinated, as their dehydration begins at much higher temperatures in comparison with $Y(Htba)_3 \cdot 8H_2O$. As "hard" acids, Ln^{3+} ions are not prone to form any bonds with the ligands through a sulfur atom, as indirectly confirmed by the crystallization of their rare complexes with S-coordinated ligands only from non-polar solvents [4]. For this reason, when considering the possible structure of the hydrates $Ln(Htba)_3 \cdot 2H_2O$ and $Ln(Htba)_3 \cdot 8H_2O$, it is possible to take into account only the Ln−O$_{Htba}$ and Ln−O$_w$ bonds. Since CN(Ln(III)) ≥ 8 in common practice, and Htba$^-$ ions do not form any O,O'-coordinated chelates [1, 2, 10], $Yb(Htba)_3 \cdot 2H_2O$ and the hydrates isostructural to it

Table 4. Crystallographic parameters of $Ln(Htba)_3 \cdot 2H_2O$ (space group $P2_12_12_1$)

Metal	a, Å	b, Å	c, Å	V, Å^3
La	6.813(1)	15.064(1)	18.326(2)	1880.9(2)
Ce	6.813(2)	15.025(2)	18.253(2)	1868.9(3)
Eu	6.742(1)	15.418(2)	18.125(2)	1883.9(3)
Yb	6.709(1)	15.325(2)	17.884(2)	1838.8(3)
Lu	6.711(1)	15.338(1)	17.882(1)	1840.7(1)
Y	6.721(1)	15.378(1)	17.982(1)	1858.5(2)
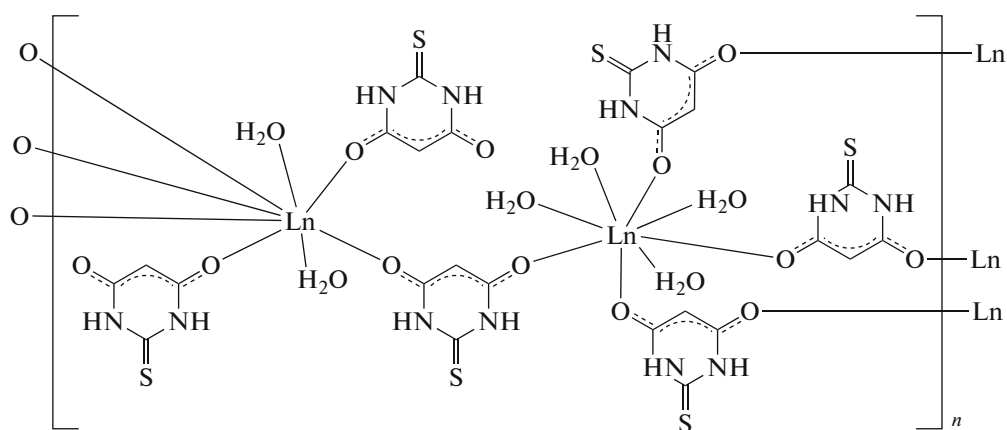
Fig. 3. Structure of $[Ln_2(H_2O)_6(HTBA-O,O')_4(HTBA-O)_2]_n$.
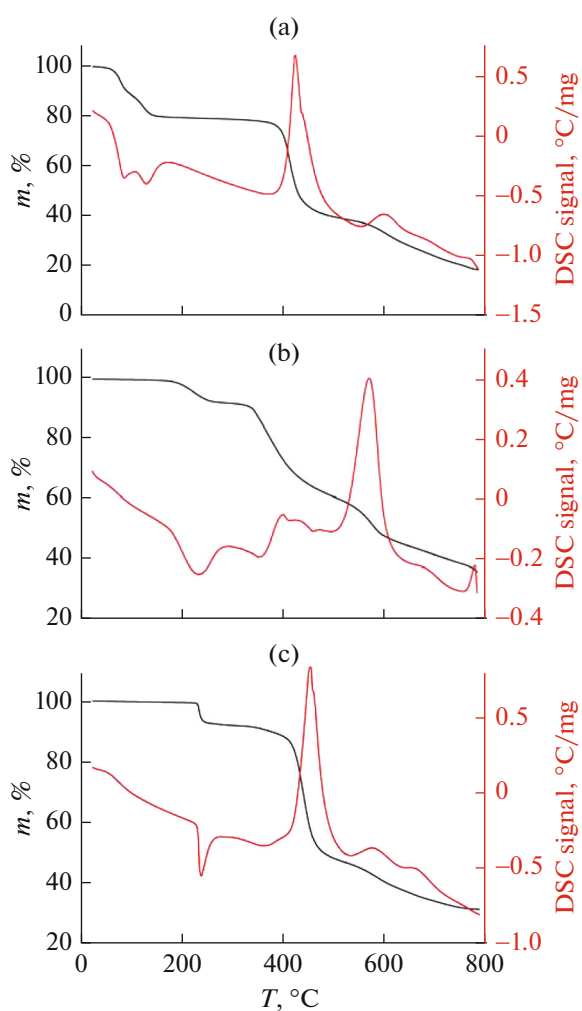
Fig. 4. TG and DSC curves for the oxidative dehydration of (a) $Y(Htba)_3 \cdot 8H_2O$, (b) $Ho(Htba)_3 \cdot 3H_2O$, and (c) $Yb(Htba)_3 \cdot 2H_2O$.

are coordination polymers. Taking into account a relatively low complete dehydration temperature typical for uncoordinated water molecules, it is also possible to presume that $Y(Htba)_3 \cdot 8H_2O$ and the complexes isostructural to it have a polymeric structure. Therefore, taking into account the earlier observed highest thermodynamic stability of $M(Htba)_3 \cdot 3H_2O$ crystals in a solution, the mutual transformations of polymeric Ln(III) hydrates in their saturated aqueous solutions can be described by the scheme

$$[Ln(Htba)_3]_n \cdot 8nH_2O \xrightarrow{1-3 \text{ months}} [Ln(H_2O)_3(Htba)_2]_n$$

$$90°C \searrow \qquad \nearrow \begin{array}{c} 1-3 \text{ months} \\ 20-25°C \end{array}$$

$$[Ln(H_2O)_2(Htba)_2]_n$$
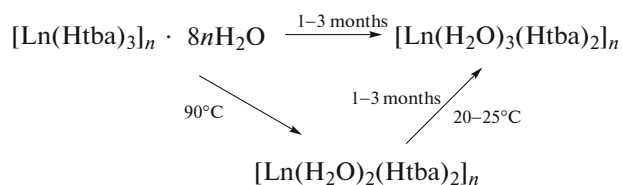
CONCLUSIONS

Three types of hydrates of thiobarbiturate REE complexes $(Htba)_3 \cdot nH_2O$ ($n = 2, 3, 8$) with different crystal structures and thermal stabilities in the processes of dehydration have been crystallized from aqueous solution under different conditions. The oxidative decomposition of coordinated $Htba^-$ ligands is started at a higher temperature than for free H_2tba, which melts with decomposition as soon as ~250°C [22].

As already mentioned, hydrates of different composition and structure were synthesized earlier for neutral homogeneous complexes formed by H_2tba and HDetba with *s*, *p*, and *d* metals (Table S1) [3]. The existence of several hydrates along with the possibility of formation of bond isomers by polyfunctional ligands enriches the coordination chemistry of the metal complexes with barbituric acids [2]. The separation of dihydrates, trihydrates, and octahydrates of REE thiobarbiturates is an example of the structural and hydrate variety of compounds of this class.

ACKNOWLEDGMENTS

FUNDING

CONFLICT OF INTERESTS

The authors declare that they have no conflict of interests.

SUPPLEMENTARY MATERIALS

Supplementary materials for this article are available to authorized users at https://doi.org/10.1134/S0036023620070098.

Table S1. Hydrates of metal barbiturate complexes [3].

Table S2. Selected bond lengths (Å) and abond angles (deg) in compounds **I−III**.

Table S3. Hydrogen bond geometry parameters in structures **I−III**.

Table S4. Htba− π−π-interaction paremeters in crystals **I−III**.

Fig. S1. Structure of a layer normal to direction $a + c$. The cylic structural fragment is indicated by a wide line.

REFERENCES

1. K. T. Mahmudov, M. N. Kopylovich, A. M. Maharramov, et al., Coord. Chem. Rev. **265**, 1 (2014).
https://doi.org/10.1016/j.ccr.2014.01.002

2. N. N. Golovnev and M. S. Molokeev, *2-Thiobarbituric Acid and Its Metal Complexes: Synthesis, Structure, and Properties* (Sib. Feder. Univ., Krasnoyarsk, 2014) [in Russian].

3. N. N. Golovnev, M. S. Molokeev, and M. K. Lesnikov, Zh. Sibirsk. Fed. Univ., Khim., No. 10, 401 (2017).
https://doi.org/10.17516/1998-2836-0036

4. S. Cotton, *Lanthanide and Actinide Chemistry* (Wiley, Rutland (UK), 2006).

5. M. C. Heffern, L. M. Matosziuk, and T. J. Meade, Chem. Rev. **114**, 4496 (2014).
https://doi.org/10.1021/cr400477t

6. Y. Yang, Q. Zhao, W. Feng, and F. Li, Chem. Rev. **113**, 192 (2013).
https://doi.org/10.1021/cr2004103

7. K. Binnemans, Chem. Rev. **109**, 4283 (2009).
https://doi.org/10.1021/cr8003983

8. N. N. Golovnev and M. S. Molokeev, Russ. J. Coord. Chem. **40**, 648 (2014).
https://doi.org/10.1134/S1070328414090036

9. N. N. Golovnev, M. S. Molokeev, and I. V. Sterkhova, Zh. Neorg. Khim. **64**, 965 (2019).
https://doi.org/10.1134/S0044457X19090137

10. Cambridge Structural Database, Version 5.37 (Univ. of Cambridge, Cambridge (UK), 2015).

11. G. M. Sheldrick, SADABS, Version 2.01 (Bruker, Madison, WI, 2004).

12. G. M. Sheldrick, SHELXTL, Version 6.10 (Bruker, Madison, WI, 2004).

13. Bruker AXS TOPAS V4: General Profile and Structure Analysis Software for Powder Diffraction Data. User's Manual (Bruker, Karlsruhe, 2008).

14. V. I. Balas, I. I. Verginadis, G. D. Geromichalos, et al., Eur. J. Med. Chem. **46**, 2835 (2011).
https://doi.org/10.5517/ccv3tc3

15. M. Kubicki, A. Owczarzak, V. I. Balas, and S. K. Hadjikakou, J. Coord. Chem. **65**, 1107 (2012).
https://doi.org/10.1080/00958972.2012.660148

16. Y. Gong, Z. Hao, J. Li, et al., Dalton Trans. **42**, 6489 (2013).
https://doi.org/10.1039/C3DT32380C

17. W. M. Hutzler, E. Egert, and M. Bolte, Acta Crystallogr., Sect. C **72**, 705 (2016).
https://doi.org/10.1107/S205322961601336X

18. S. Gomathi, J. S. Nirmalram, and P. T. Muthiah, Acta Crystallogr., Sect. B **71**, 144 (2015).
https://doi.org/10.1107/S2052520615001729

19. C. Wang, M.-S. Zhou, L.-J. Yang, et al., Jiegou Huaxue **36**, 1210 (2017).
https://doi.org/10.14102/j.cnki.0254-5861.2011-1494

20. J. W. Steed and J. L. Atwood *Supramolecular Chemistry* 1st Ed. (CRC Press, 2004; Akademkniga, Moscow, 2007).

21. PLATON: A Multipurpose Crystallographic Tool (Utrecht Univ., Utrecht, The Netherlands, 2008).

22. M. V. Roux, R. Notario, M. Segura, and J. S. Chickos, J. Chem. Eng. Data **57**, 249 (2011).
https://doi.org/10.1021/je200420u

Translated by E. Glushachenkova